R2-based Hypervolume Contribution Approximation

Ke Shang, Hisao Ishibuchi, *Fellow, IEEE,* and Xizi Ni

***Abstract*—In this paper, a new hypervolume contribution approximation method is proposed which is formulated as an R2 indicator. The basic idea of the proposed method is to use different line segments only in the hypervolume contribution region for the hypervolume contribution approximation. Compared with a traditional method which is based on the R2 indicator to approximate the hypervolume, the new method can directly approximate the hypervolume contribution and will utilize all the direction vectors only in the hypervolume contribution region. The new method, the traditional method and the Monte Carlo sampling method are compared through numerical experiments. Our experimental results show the superiority of the new method over the other two methods, where the new method achieves the best performance for comparing hypervolume contributions of different solutions and identifying the solution with the smallest hypervolume contribution.**

***Index Terms*—Hypervolume contribution, R2 indicator, Evolutionary multi-objective optimization.**

I. Introduction

Hypervolume [1] is a widely used performance indicator in the Evolutionary Multi-objective Optimization (EMO) community due to its well-known unique property (i.e., Pareto compliance) among all the existing indicators. The bottleneck of the hypervolume applicability in Evolutionary Multi-objective Optimization Algorithms (EMOA) is the increasing computational burden as the dimensionality of the objective space increases. Whereas several fast hypervolume calculation methods [2], [3], [4] have been proposed, it has been proved that the exact hypervolume calculation is #P-hard in the number of dimensions [5]. Therefore, efforts in the hypervolume approximation have been done to increase the applicability of the hypervolume to high-dimensional spaces, including the Monte Carlo sampling method [6], [7], [8] and the achievement scalarizing function method [9], [10].

In the achievement scalarizing function method, the hypervolume is approximated by a number of achievement scalarizing functions with uniformly distributed weight vectors. Each achievement scalarizing function with a different weight vector is used to measure the distance from the reference point to the attainment surface of the solution set. Then the average distance from the reference point to the attainment surface over a large number of weight vectors is calculated as the hypervolume approximation.

The achievement scalarizing function method can be formulated as an R2 indicator. In [11], an R2 indicator is proposed based on a new Tchebycheff function. The proposed R2 indicator shows a clear geometric property to approximate the hypervolume. In [12], a new R2 indicator is proposed based on the Divergence theorem and Riemann sum approximation for better hypervolume approximation. The new R2 indicator significantly improved the approximation quality for the hypervolume compared with the achievement scalarizing function method.

In the hypervolume-based EMOA (e.g., SMS-EMOA [13], [14]), the hypervolume contribution is used to evaluate the fitness value of each individual. With a steady-state $(\mu + 1)$ ES-type generation update mechanism, the worst individual with the smallest hypervolume contribution is eliminated from the population. Thus, the hypervolume contribution plays an important role in the hypervolume-based EMOA. This paper investigates hypervolume contribution approximation methods based on the R2 indicator. The main contribution of this paper is that a new method which is formulated as an R2 indicator is proposed for the hypervolume contribution approximation. Compared with a traditional method which is based on the R2 indicator to approximate the hypervolume, the new method can directly approximate the hypervolume contribution and is able to achieve a better approximation performance with only a small number of direction vectors.

The remainder of the paper is organized as follows. Section II gives the preliminaries of the paper. R2-based hypervolume contribution approximation methods are investigated in Section III. Numerical studies are given in Section IV. We conclude the paper in Section V.

II. Preliminaries

A. Hypervolume and hypervolume contribution

Given a reference point $\mathbf{r}$ and an approximation solution set A, the hypervolume of the set A is defined as:

$$HV(A, \mathbf{r}) = \mathcal{L}\left(\bigcup_{\mathbf{a}\in A} \{\mathbf{b} | \mathbf{a} \succ \mathbf{b} \succ \mathbf{r}\}\right), \tag{1}$$

where $\mathcal{L}(.)$ is the Lebesgue measure of a set, and $\mathbf{a} \succ \mathbf{b}$ means $\mathbf{a}$ dominates $\mathbf{b}$.

For a solution $\mathbf{s} \in A$, its hypervolume contribution is defined as:

$$C_{HV}(\mathbf{s}, A, \mathbf{r}) = HV(A, \mathbf{r}) - HV(A \setminus \{\mathbf{s}\}, \mathbf{r}). \tag{2}$$

Fig. 1 gives an illustration of the hypervolume of a solution set and the hypervolume contribution of each solution. The hypervolume is the shaded area of the enclosed polygon in Fig. 1 (a). The hypervolume contribution of each solution is the shaded area which is uniquely dominated by the corresponding solution in Fig. 1 (b).

K. Shang, H. Ishibuchi, and X. Ni are with Shenzhen Key Laboratory of Computational Intelligence, University Key Laboratory of Evolving Intelligent Systems of Guangdong Province, Department of Computer Science and Engineering, Southern University of Science and Technology, Shenzhen 518055, China (e-mail: kshang@foxmail.com; hisao@sustc.edu.cn; francis.x.ni@gmail.com).

Manuscript received XXX; revised XXX.

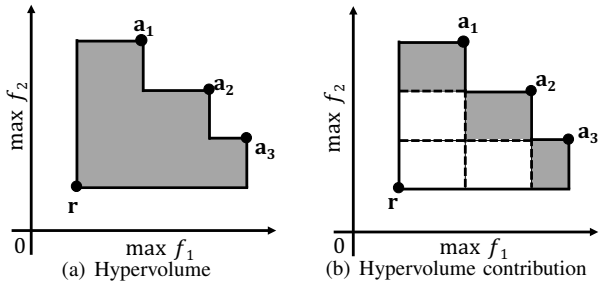

Fig. 1. An illustration of the hypervolume and the hypervolume contribution

B. R2 indicator for hypervolume approximation

Given a solution set A, a set of direction vectors Λ, and a utopian point $\mathbf{r}^*$, the R2 indicator based on the 2-Tch function [11] is defined for an m-objective problem as:

$$R_2^{2tch}(A,\Lambda,\mathbf{r}^*)=\frac{1}{|\Lambda|}\sum_{\lambda\in\Lambda}\min_{\mathbf{a}\in A}\left\{g^{2tch}(\mathbf{a}|\lambda,\mathbf{r}^*)\right\}, \quad (3)$$

where the 2-Tch function is defined as follows:

$$g^{2tch}(\mathbf{a}|\lambda,\mathbf{r}^*)=\max_{j\in\{1,\ldots,m\}}\left\{\frac{|r_j^*-a_j|}{\lambda_j}\right\}. \quad (4)$$

In Eq. (4), $\lambda=(\lambda_1,\lambda_2,...,\lambda_m)$ is a given direction vector with $\|\lambda\|_2=1$ and $\lambda_i\geq 0$, $i=1,...,m$.

Fig. 2 (a) shows the geometric property of R_2^{2tch}. In this figure, $\mathbf{r}^*$ is the utopian point and $\mathbf{r}$ is the reference point for the hypervolume calculation. Suppose a line follows the direction λ and passes through $\mathbf{r}^*$ and intersects with the attainment surface of the solution set A at $\mathbf{p}$, then the length of the line segment with the end points $\mathbf{r}^*$ and $\mathbf{p}$ is determined by $\min_{\mathbf{a}\in A}\left\{g^{2tch}(\mathbf{a}|\lambda,\mathbf{r}^*)\right\}$. R_2^{2tch} in Eq. (3) is the average length of the line segments with different directions as shown in Fig. 2 (a).

The idea of using different line segments starting from a reference point to the attainment surface of the solution sets for the hypervolume approximation was firstly proposed in [9] as shown in Fig. 2 (b). Intuitively, the average length of the line segments in Fig. 2 (b) is closely related to the hypervolume.

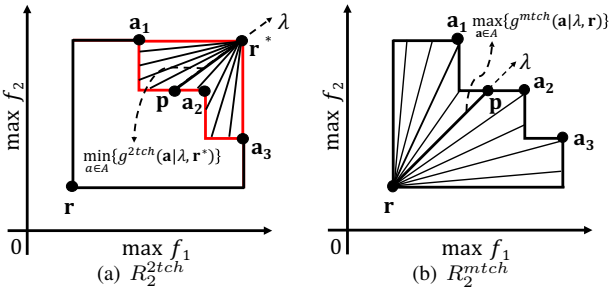

Fig. 2. An illustration of the geometric property of R_2^{2tch} and R_2^{mtch}.

The R_2^{2tch} indicator cannot be directly used for the hypervolume approximation as shown in Fig. 2 (a). Its modified version which is able to directly approximate the hypervolume is defined as follows:

$$R_2^{mtch}(A,\Lambda,\mathbf{r})=\frac{1}{|\Lambda|}\sum_{\lambda\in\Lambda}\max_{\mathbf{a}\in A}\left\{g^{mtch}(\mathbf{a}|\lambda,\mathbf{r})\right\}, \quad (5)$$

where g^{mtch} function is defined as follows:

$$g^{mtch}(\mathbf{a}|\lambda,\mathbf{r})=\min_{j\in\{1,\ldots,m\}}\left\{\frac{|r_j-a_j|}{\lambda_j}\right\}. \quad (6)$$

In Eq. (6), $\mathbf{r}$ is the reference point for the hypervolume calculation, λ is a given direction vector which is the same as in g^{2tch} in Eq. (4).

It is easy to show that the R_2^{mtch} indicator has a geometric property as shown in Fig. 2 (b), which can be used directly for the hypervolume approximation.

In our previous work [12], a new R2 indicator is proposed for better hypervolume approximation. The new R2 indicator is derived based on the Divergence theorem and Riemann sum approximation. It is defined as follows:

$$R_2^{HV}(A,\Lambda,\mathbf{r})=\frac{1}{|\Lambda|}\sum_{\lambda\in\Lambda}\max_{\mathbf{a}\in A}\left\{g^{mtch}(\mathbf{a}|\lambda,\mathbf{r})\right\}^m. \quad (7)$$

Comparing Eq. (7) with Eq. (5), we can see that the only difference between R_2^{mtch} and R_2^{HV} is the added exponential m in R_2^{HV}. This small change in R_2^{HV} significantly improves the approximation quality of the R2 indicator for the hypervolume. For detailed explanations of the new R2 indicator, please refer to our previous work [12].

III. R2-BASED HYPERVOLUME CONTRIBUTION APPROXIMATION

A. Traditional method and its drawbacks

As shown in the previous section, the R2 indicator (e.g., R_2^{mtch} and R_2^{HV}) can be used to approximate the hypervolume. We can also use the R2 indicator to approximate the hypervolume contribution. The simplest and straightforward method is to use the R2 contribution to approximate the hypervolume contribution.

For a solution $\mathbf{s}\in A$, its R2 contribution is defined as follows:

$$C_{R_2}(\mathbf{s},A,\Lambda,\mathbf{r})=R_2(A,\Lambda,\mathbf{r})-R_2(A\setminus\{\mathbf{s}\},\Lambda,\mathbf{r}), \quad (8)$$

where R_2 can be R_2^{mtch} and R_2^{HV} for the hypervolume approximation.

According to the definition of the R2 contribution, the traditional method for the hypervolume contribution approximation (as illustrated in Fig. 3) can be described by the following three steps:

- Step 1: Calculate the R2 value of the solution set A.
- Step 2: Calculate the R2 value of the solution set $A\setminus\{\mathbf{s}\}$.
- Step 3: Calculate the difference between the above two R2 values as the hypervolume contribution approximation of the solution $\mathbf{s}$.

The drawbacks of the traditional method are summarized as follows:

1) In order to obtain the hypervolume contribution approximation of a solution, we need to calculate R2 values for

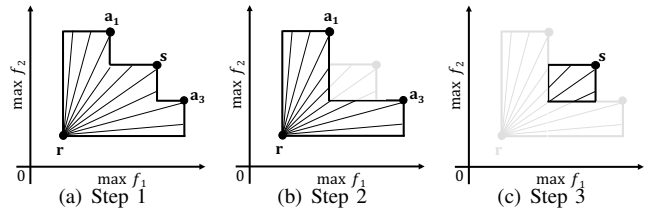

Fig. 3. An illustration of the traditional method for the hypervolume contribution approximation. The hypervolume contribution of solution $\mathbf{s}$ is approximated by the difference between the R2 values of the solution sets $\{\mathbf{a}_1, \mathbf{s}, \mathbf{a}_3\}$ and $\{\mathbf{a}_1, \mathbf{a}_3\}$.

two solution sets. The hypervolume contribution cannot be approximated directly.

2) Usually there exist errors in the R2 approximation for the hypervolume. So the error of the hypervolume contribution approximation could be amplified by the errors of the two R2 values. For this reason, the approximation accuracy of the traditional method may be low.
3) In order to improve the approximation accuracy, a large number of vectors are needed for calculating the R2 indicator. Thus, the amount of computation in the traditional method could be large so as to achieve a high approximation accuracy.

B. A new method for hypervolume contribution approximation

In this subsection, a new method is proposed for the hypervolume contribution approximation. The basic idea is to use different line segments only in the hypervolume contribution region for the hypervolume contribution approximation.

The proposed idea is illustrated in Fig. 4 (a). In Fig. 4 (a), the hypervolume contribution region of a solution $\mathbf{s}$ is occupied by the line segments with different directions which start from the solution $\mathbf{s}$ and end on the boundaries of the hypervolume contribution region of the solution $\mathbf{s}$. Then we can utilize all the line segments in the hypervolume contribution region to approximate the corresponding hypervolume contribution, which is similar to R_2^{mtch} or R_2^{HV} for the hypervolume approximation.

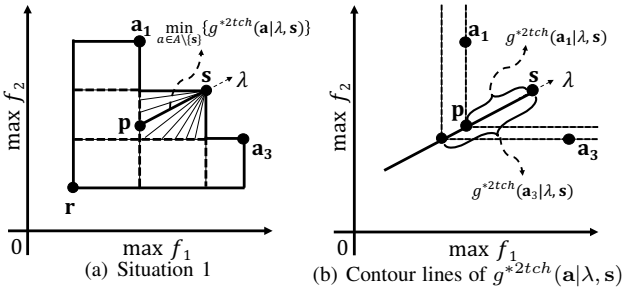

Fig. 4. An illustration of the proposed idea (Situation 1).

First, let us consider the situation in Fig. 4 (a). In this situation, the line segments in the hypervolume contribution region of the solution $\mathbf{s}$ only intersect with the attainment surface of the solution set $A \setminus \{\mathbf{s}\}$, i.e., the lengths of the line segments are only determined by the solution set $A \setminus \{\mathbf{s}\}$. This situation is similar to R_2^{2tch} as illustrated in Fig. 2 (a).

Given a direction vector λ, a solution $\mathbf{s}$ and a solution set $A \setminus \{\mathbf{s}\}$, the length of the line segment in Fig. 4 (a) can be calculated by the following formula:

$$L(\mathbf{s}, A, \lambda) = \min_{\mathbf{a} \in A \setminus \{\mathbf{s}\}} \left\{ g^{*2tch}(\mathbf{a}|\lambda, \mathbf{s}) \right\}. \tag{9}$$

In Eq. (9), the $g^{*2tch}(\mathbf{a}|\lambda, \mathbf{s})$ function is defined for maximization problems as

$$g^{*2tch}(\mathbf{a}|\lambda, \mathbf{s}) = \max_{j \in \{1,\ldots,m\}} \left\{ \frac{s_j - a_j}{\lambda_j} \right\}, \tag{10}$$

For minimization problems, it is defined as

$$g^{*2tch}(\mathbf{a}|\lambda, \mathbf{s}) = \max_{j \in \{1,\ldots,m\}} \left\{ \frac{a_j - s_j}{\lambda_j} \right\}. \tag{11}$$

In the maximization case which is considered in Fig. 4 (a), notice that $g^{*2tch}(\mathbf{a}|\lambda, \mathbf{s})$ is slightly different from $g^{2tch}(\mathbf{a}|\lambda, \mathbf{r}^*)$ in Eq. (4) that there is no absolute value sign in $g^{*2tch}(\mathbf{a}|\lambda, \mathbf{s})$ in Eq. (10). The reason can be clearly explained by Fig. 4 (b), which shows the contour lines of $g^{*2tch}(\mathbf{a}|\lambda, \mathbf{s})$ in the maximization case. If the absolute value sign is added in $g^{*2tch}(\mathbf{a}|\lambda, \mathbf{s})$, then the contour line property will be changed and the lengths of the line segments may not be correctly calculated. The same analysis can be applied to $g^{*2tch}(\mathbf{a}|\lambda, \mathbf{s})$ in the minimization case.

Next, let us consider the situation in Fig. 5 (a). In this situation, the line segments in the hypervolume contribution region of the solution $\mathbf{s}$ not only intersect with the attainment surface of the solution set $A \setminus \{\mathbf{s}\}$ but also intersect with the hypervolume boundary of the solution set A associated with the reference point $\mathbf{r}$. For the line segments intersecting with the attainment surface of the solution set $A \setminus \{\mathbf{s}\}$, the lengths can be calculated by Eq. (9). For the line segments intersecting with the hypervolume boundary associated with the reference point $\mathbf{r}$, the lengths are calculated as follows:

$$L(\mathbf{s}, \mathbf{r}, \lambda) = g^{mtch}(\mathbf{r}|\lambda, \mathbf{s}), \tag{12}$$

where $g^{mtch}(\mathbf{r}|\lambda, \mathbf{s})$ is defined as:

$$g^{mtch}(\mathbf{r}|\lambda, \mathbf{s}) = \min_{j \in \{1,\ldots,m\}} \left\{ \frac{|s_j - r_j|}{\lambda_j} \right\}. \tag{13}$$

Fig. 5 (b) and (c) show the contour lines of $g^{mtch}(\mathbf{r}|\lambda, \mathbf{s})$ in Eq. (13) and $g^{*2tch}(\mathbf{a}|\lambda, \mathbf{s})$ in Eq. (10) respectively. From Fig. 5 (b) for a line segment intersecting with the hypervolume boundary associated with the reference point $\mathbf{r}$, its length is $L(\mathbf{s}, \mathbf{r}, \lambda_1)$ and $L(\mathbf{s}, \mathbf{r}, \lambda_1) < L(\mathbf{s}, A, \lambda_1)$ holds. From Fig. 5 (c) for a line segment intersecting with the attainment surface of the solution set $A \setminus \{\mathbf{s}\}$, its length is $L(\mathbf{s}, A, \lambda_2)$ and $L(\mathbf{s}, A, \lambda_2) < L(\mathbf{s}, \mathbf{r}, \lambda_2)$ holds.

Wrapping up the above two situations, the length of any line segment along the direction λ starting from $\mathbf{s}$ and intersecting with the boundaries of the hypervolume contribution region is calculated as follows:

$$L(\mathbf{s}, A, \mathbf{r}, \lambda) = \min\{L(\mathbf{s}, A, \lambda), L(\mathbf{s}, \mathbf{r}, \lambda)\}. \tag{14}$$

Based on the lengths of the line segments in the hypervolume contribution region, we can define the following R2

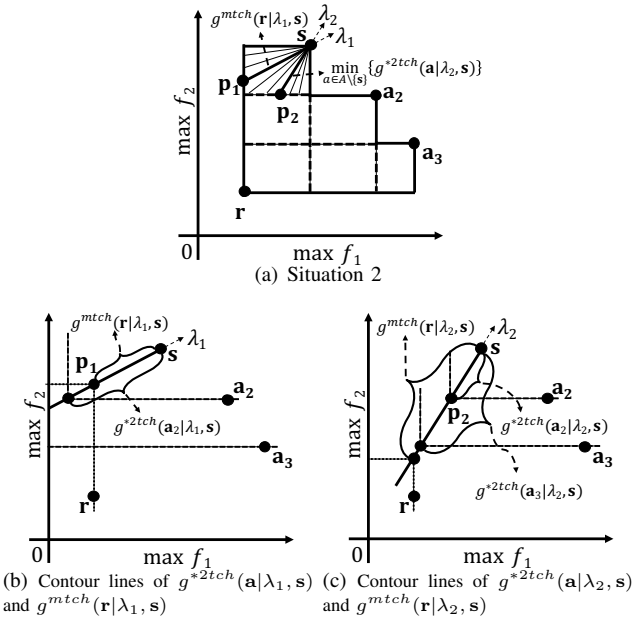

(a) Situation 2

(b) Contour lines of $g^{*2tch}(\mathbf{a}|\lambda_1,\mathbf{s})$ and $g^{mtch}(\mathbf{r}|\lambda_1,\mathbf{s})$

(c) Contour lines of $g^{*2tch}(\mathbf{a}|\lambda_2,\mathbf{s})$ and $g^{mtch}(\mathbf{r}|\lambda_2,\mathbf{s})$

Fig. 5. An illustration of the proposed idea (Situation 2).

indicator to approximate the hypervolume contribution:

$$R_2^{HVC}(\mathbf{s},A,\Lambda,\mathbf{r}) = \frac{1}{|\Lambda|}\sum_{\lambda\in\Lambda} L\left(\mathbf{s},A,\mathbf{r},\lambda\right)^{\alpha}$$
$$= \frac{1}{|\Lambda|}\sum_{\lambda\in\Lambda}\min\left\{\min_{\mathbf{a}\in A\setminus\{\mathbf{s}\}}\left\{g^{*2tch}(\mathbf{a}|\lambda,\mathbf{s})\right\}, g^{mtch}(\mathbf{r}|\lambda,\mathbf{s})\right\}^{\alpha}, \tag{15}$$

where $\alpha = 1$ if we want to use the average length of the line segments for the approximation, or $\alpha = m$ if we want to use the average m powered length of the line segments for the approximation.

Compared with the traditional method described in the previous subsection, the proposed new method for the hypervolume contribution approximation has the following advantages:

1) The hypervolume contribution approximation of a solution can be directly calculated by Eq. (15).
2) The new method will utilize all direction vectors only in the hypervolume contribution region, while the traditional method utilizes them across the entire hypervolume region. For this reason, the approximation accuracy of the new method could be much higher than the traditional method when the same number of direction vectors are used in each method.

IV. Numerical studies

A. Experiment settings

1) Solution sets generation: In our experiments, we examine six types of Pareto front (PF): triangular PF (including linear, convex and concave) and inverted triangular PF (including linear, convex and concave). For the triangular PF, the linear PF is expressed as $f_1 + f_2 + ... + f_m = 1$ and $f_i \geq 0$ for $i = 1, ..., m$, the concave PF is expressed as $f_1^2 + f_2^2 + ... + f_m^2 = 1$ and $f_i \geq 0$ for $i = 1, ..., m$, the convex PF is expressed as $\sqrt{f_1} + \sqrt{f_2} + ... + \sqrt{f_m} = 1$ and $f_i \geq 0$ for $i = 1, ..., m$. For the inverted triangular PF, it is obtained by transforming each point of the triangular PF by $1 - f_i$ for $i = 1, ..., m$.

We examine 5-dimension and 10-dimension cases (i.e., $m = 5, 10$). For each case, 100 solutions are randomly sampled from each PF to form solution sets with different PF shapes. This sampling procedure is repeated to generate 100 solution sets for each PF shape.

The maximization case is considered. The reference point $\mathbf{r} = (r, ..., r) \in \mathbb{R}^m$ is set as $r = 0.0, -0.1, ..., -0.4$.

2) Compared methods: Three methods for the hypervolume contribution approximation are compared. The first method is the traditional method described in Section III-A. The second method is the new method proposed in Section III-B. The third method is the Monte Carlo sampling method proposed in [6]. In this method, the tightest sampling space of a solution is determined first, then the samples are drawn in this sampling space to estimate the hypervolume contribution of the corresponding solution. More detailed explanations of the Monte Carlo sampling method can be found in [6].

For the traditional method, we use R_2^{HV} (Eq. (7)) as the R2 indicator and approximate the hypervolume contribution according to the R2 contribution (Eq. (8)). For the new method, we use R_2^{HVC} (Eq. (15)) for the approximation and choose $\alpha = m$. The direction vectors used in the R2 indicator are generated by uniformly sampling points on the unit hypersphere[1], while the sampling points used in the Monte Carlo method are uniformly sampled in the sampling space.

In order to investigate the effect of the number of the direction vectors and the sampling points on the performance of the three methods, we examine ten settings: $100, 200, ..., 1000$ direction vectors and sampling points.

B. Performance metrics

Two performance metrics are used to evaluate the performance of the three methods for the hypervolume contribution approximation.

The first metric is the consistency rate in the order of the solution pairs in the solution set between their true hypervolume contributions and their approximated hypervolume contributions. Given a solution set A, there are a total number of $\binom{|A|}{2}$ solution pairs. For two solutions $\mathbf{s}_1$ and $\mathbf{s}_2$ from A, if the orders of their true hypervolume contributions and their approximated hypervolume contributions are the same, then the solution pair $(\mathbf{s}_1, \mathbf{s}_2)$ is called a consistent pair. The consistency rate of a solution set A is the ratio of the total number of the consistent pairs to $\binom{|A|}{2}$.

The second metric is the correct identification rate of the worst solution with the smallest hypervolume contribution in each solution set over all solution sets. For a solution set, if the solution with the smallest approximated hypervolume contribution also has the smallest true hypervolume contribution, then we call it as a correct identification for this solution set. The correct identification rate is the ratio of the total number

[1]First we randomly sample a points $\mathbf{x}$ according to the normal distribution $\mathcal{N}_m(0, I_m)$, then the corresponding direction vector is obtained by $\lambda = |\mathbf{x}|/\|\mathbf{x}\|_2$.

of the correct identifications to the total number of the solution sets.

For each type of solution sets (e.g., 5-dimension solution sets with the linear triangular PF), there are a total number of 100 solution sets. First the consistency rate for each solution set is calculated and then the average over the 100 solution sets is obtained. The correct identification rate is determined by the proportion of the correct identification solution sets in the 100 solution sets.

C. Results analysis

The results of the two performance metrics on 5-dimension solution sets are shown in Fig. 6-11. All the results shown in the figures are the average of 30 independent runs with different seeds in the generation of the direction vectors and the sampling points. The x-axis is the number of the direction vectors for the traditional and the new methods, or the number of the sampling points for the Monte Carlo sampling method.

For the triangular PF solution sets (see Fig. 6-8), we can observe that the new method always outperforms the traditional method in terms of both performance metrics. When the reference point $r = 0.0$, the Monte Carlo method shows the best performance, while its performance deteriorates dramatically as the reference point changes from 0.0 to -0.4. The new method shows a robust performance with respect to the specification of the reference point. Its performance is worse than the Monte Carlo method only when $r = 0.0$, while it outperforms the Monte Carlo method when $r = -0.1, ..., -0.4$.

For the inverted triangular PF solution sets (see Fig. 9-11), we can observe that the new method always outperforms the traditional method and the Monte Carlo method in terms of both performance metrics. We can also see that the new method achieves a robust performance with respect to the specification of the reference point.

For both cases (i.e., the triangular and the inverted triangular PF solution sets), we can see that the new method is able to achieve a good performance even when the number of the direction vectors is small (e.g., 100). This is because the new method uses all the direction vectors in the hypervolume contribution region, which is also one advantage of the new method compared with the traditional method.

The reason why the Monte Carlo method achieves a very good performance on the triangular PF solution sets when $r = 0.0$ (while its performance deteriorates dramatically when $r = -0.1, ..., -0.4$) can be explained as follows: If $r = 0.0$, all solutions on the PF boundaries will have zero hypervolume contributions [15]. So the solution with the smallest hypervolume contribution tends to lie close to the PF boundaries. In this case, the solution with the smallest hypervolume contribution tends to have a small sampling space compared with other solutions, which makes the Monte Carlo method easy to identify it. When $r = -0.1, ..., -0.4$, all solutions on the PF boundaries will have nonzero hypervolume contributions and their hypervolume contributions will increase as the reference point moves further [15]. As a result, the solution with the smallest hypervolume contribution tends to lie inside of the PF. In this case, the sampling space for the solution with the smallest hypervolume contribution tends to have similar size to other solutions, which makes the Monte Carlo method difficult to identify it. We give some detailed examples to clearly explain this phenomenon in the supplementary material.

From the experiment results we can conclude that: (1) The advantage of the new method over the traditional method is that the new method utilizes all the direction vectors in the hypervolume contribution region, which makes the new method achieving a good performance even when the number of the direction vectors is small. (2) The advantage of the new method over the Monte Carlo method is that the new method has a robust and stable performance with respect to the specification of the reference point, which is more practical in the hypervolume-based EMOAs.

Due to the page limitation, we do not show the experiment results on the 10-dimension solution sets. They are provided in the supplementary material. Similar observations are obtained from our computational experiments on the 10-dimension solution sets.

V. Conclusions

In this paper, a new method for the hypervolume contribution approximation was proposed. The experimental results showed the superiority of the new method over the other two methods for the hypervolume contribution approximation. The proposed method will bring opportunities for the development of new indicator-based EMOAs. One future research direction is to develop such an indicator-based EMOA and compare it with the hypervolume-based EMOAs [14], [7] and other R2 indicator-based EMOAs [16], [17], [18]. Another future research direction is to further improve the approximation performance of the proposed method.

The solution sets and the source code of our experiments are available at https://github.com/nixizi/R2-HVC.

References

[1] E. Zitzler and L. Thiele, "Multiobjective optimization using evolutionary algorithms - a comparative case study," in *international conference on parallel problem solving from nature*. Springer, 1998, pp. 292–301.

[2] L. While, L. Bradstreet, and L. Barone, "A fast way of calculating exact hypervolumes," *IEEE Transactions on Evolutionary Computation*, vol. 16, no. 1, pp. 86–95, 2012.

[3] L. M. S. Russo and A. P. Francisco, "Quick hypervolume," *IEEE Transactions on Evolutionary Computation*, vol. 18, no. 4, pp. 481–502, 2014.

[4] A. P. Guerreiro and C. M. Fonseca, "Computing and updating hypervolume contributions in up to four dimensions," *IEEE Transactions on Evolutionary Computation*, vol. 22, no. 3, pp. 449–463, 2018.

[5] K. Bringmann and T. Friedrich, "Approximating the volume of unions and intersections of high-dimensional geometric objects," *Computational Geometry Theory and Applications*, vol. 43, no. 6, pp. 601–610, 2010.

[6] J. Bader, K. Deb, and E. Zitzler, "Faster hypervolume-based search using Monte Carlo sampling," in *Multiple Criteria Decision Making for Sustainable Energy and Transportation Systems*. Springer, 2010, pp. 313–326.

[7] J. Bader and E. Zitzler, "HypE: An algorithm for fast hypervolume-based many-objective optimization," *Evolutionary computation*, vol. 19, no. 1, pp. 45–76, 2011.

[8] K. Bringmann and T. Friedrich, "Approximating the least hypervolume contributor: NP-hard in general, but fast in practice," *Theoretical Computer Science*, vol. 425, no. 2, pp. 104–116, 2012.

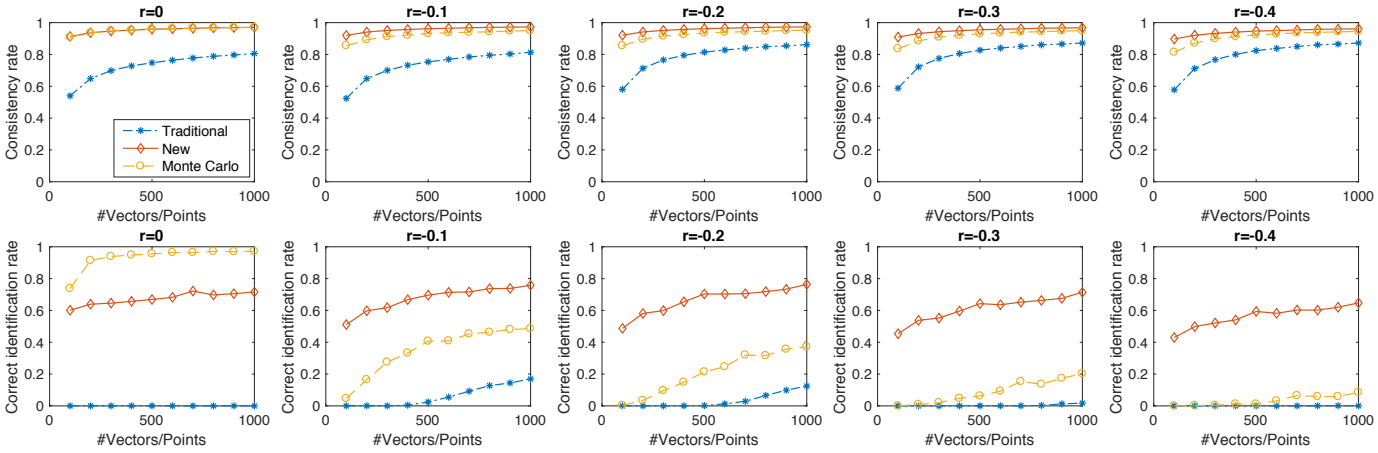

Fig. 6. Results on the 5-dimension linear triangular PF solution sets.

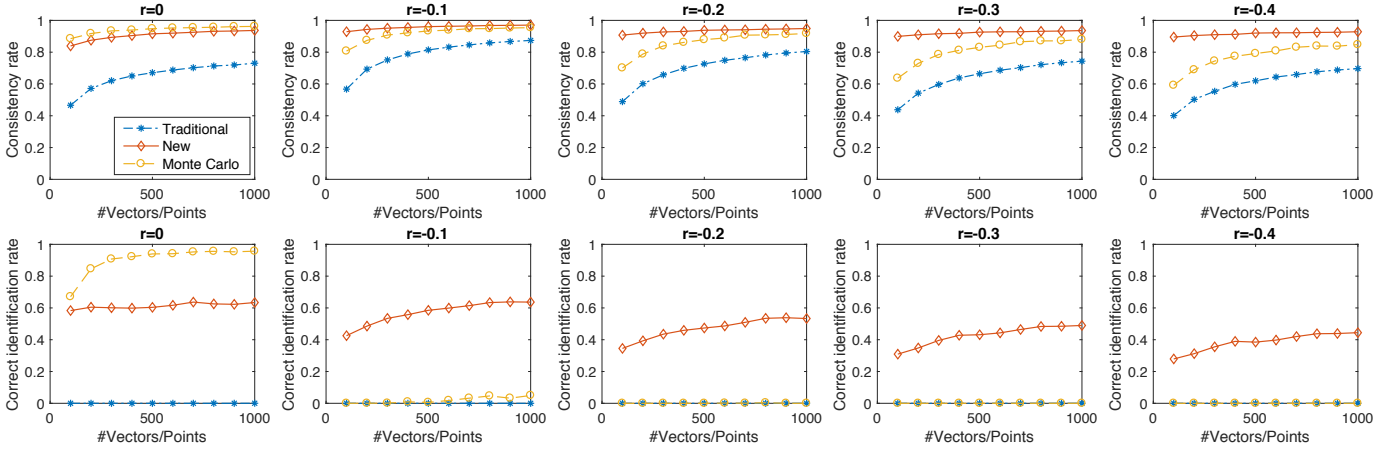

Fig. 7. Results on the 5-dimension convex triangular PF solution sets.

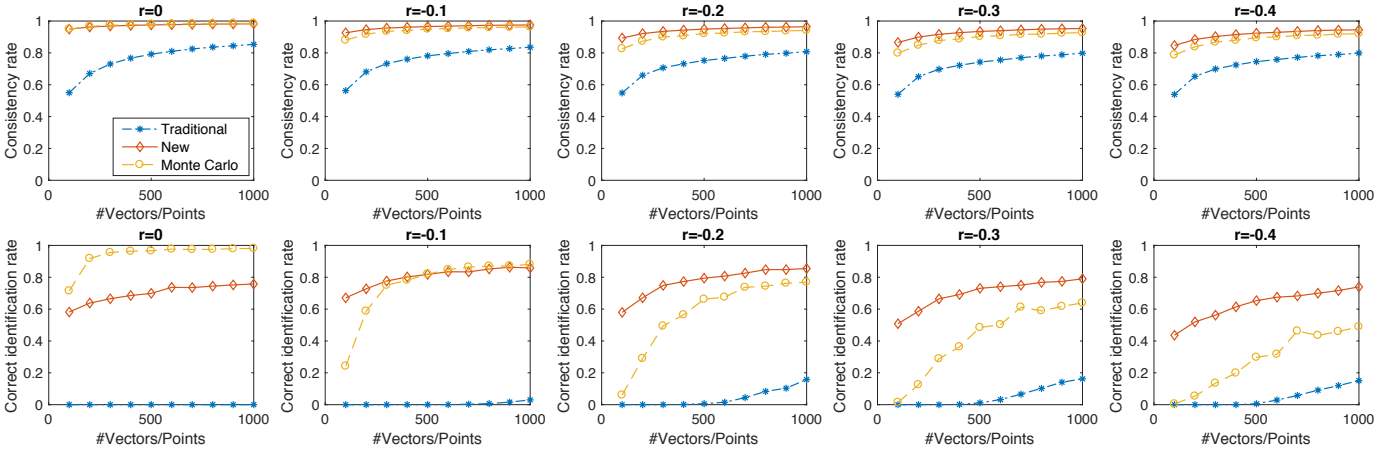

Fig. 8. Results on the 5-dimension concave triangular PF solution sets.

[9] H. Ishibuchi, N. Tsukamoto, Y. Sakane, and Y. Nojima, "Hypervolume approximation using achievement scalarizing functions for evolutionary many-objective optimization," in *Evolutionary Computation, 2009. CEC'09. IEEE Congress on*. IEEE, 2009, pp. 530–537.

[10] ——, "Indicator-based evolutionary algorithm with hypervolume approximation by achievement scalarizing functions," in *Proceedings of the 12th annual conference on Genetic and evolutionary computation*. ACM, 2010, pp. 527–534.

[11] X. Ma, Q. Zhang, G. Tian, J. Yang, and Z. Zhu, "On tchebycheff decomposition approaches for multiobjective evolutionary optimization," *IEEE Transactions on Evolutionary Computation*, vol. 22, no. 2, pp. 226–244, 2018.

[12] K. Shang, H. Ishibuchi, M.-L. Zhang, and Y. Liu, "A new R2 indicator for better hypervolume approximation," in *Proceedings of the Genetic and Evolutionary Computation Conference*, ser. GECCO '18. New York, NY, USA: ACM, 2018, pp. 745–752.

[13] M. Emmerich, N. Beume, and B. Naujoks, "An EMO algorithm using the hypervolume measure as selection criterion," in *International Con-*

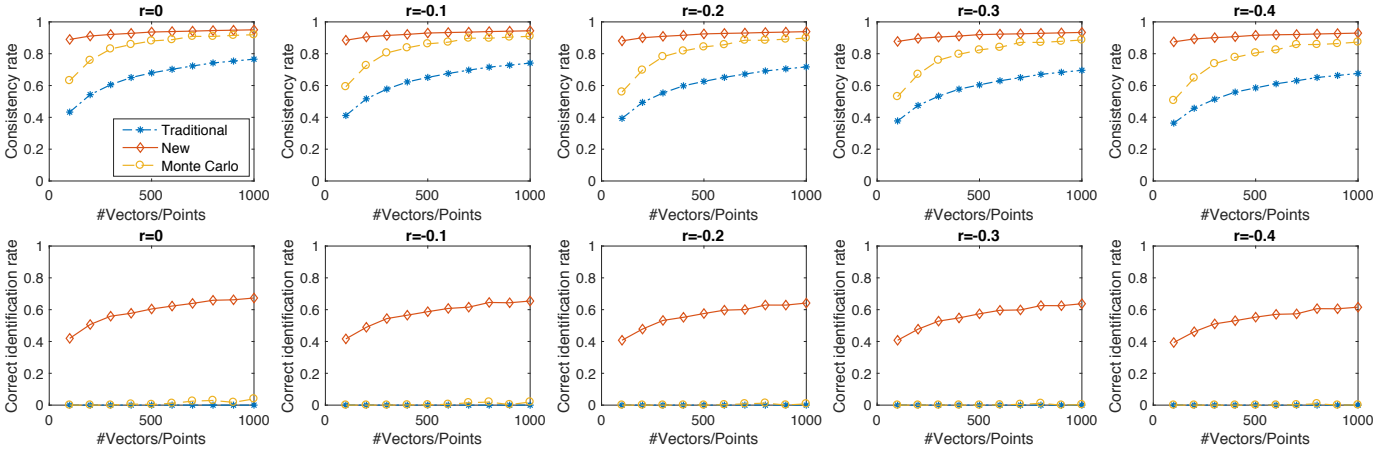

Fig. 9. Results on the 5-dimension linear inverted triangular PF solution sets.

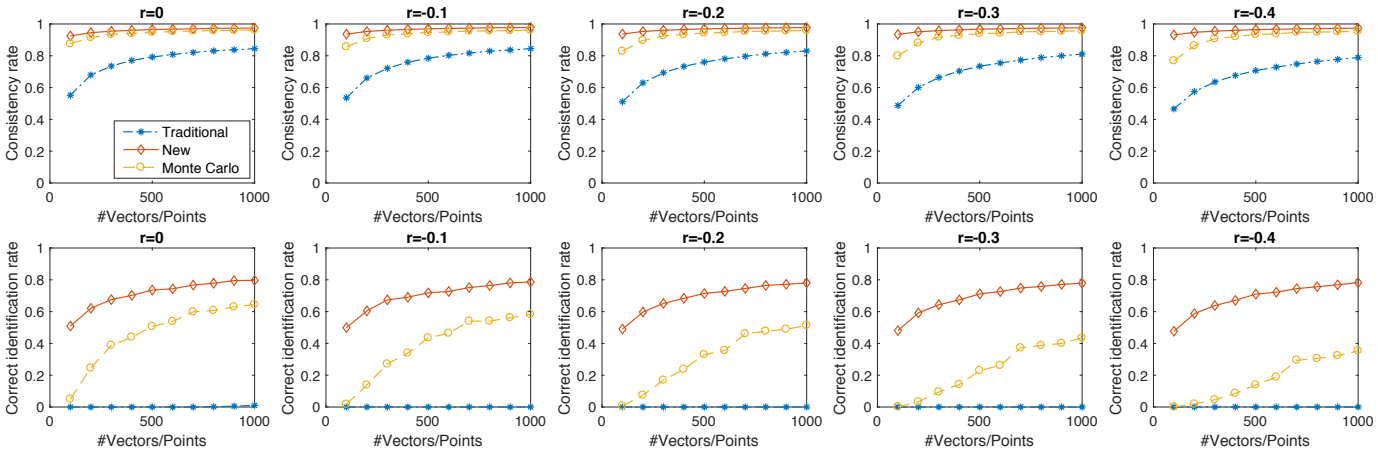

Fig. 10. Results on the 5-dimension convex inverted triangular PF solution sets.

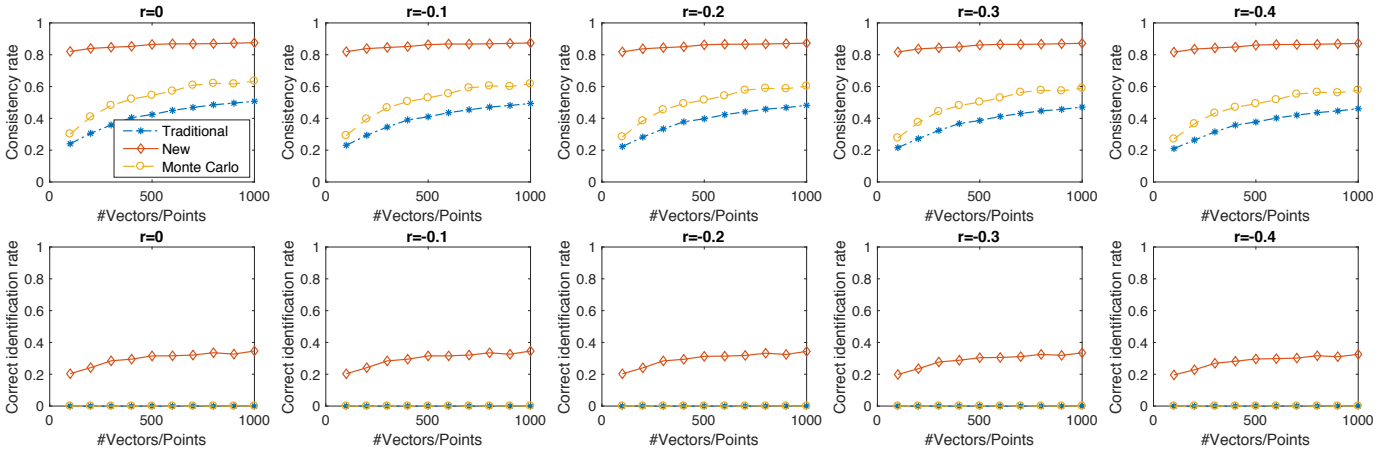

Fig. 11. Results on the 5-dimension concave inverted triangular PF solution sets.

ference on Evolutionary Multi-Criterion Optimization, 2005, pp. 62–76.

[14] N. Beume, B. Naujoks, and M. Emmerich, "SMS-EMOA: Multiobjective selection based on dominated hypervolume," *European Journal of Operational Research*, vol. 181, no. 3, pp. 1653–1669, 2007.

[15] H. Ishibuchi, R. Imada, Y. Setoguchi, and Y. Nojima, "How to specify a reference point in hypervolume calculation for fair performance comparison." *Evolutionary Computation*, vol. 26, no. 3, pp. 411–440, 2018.

[16] D. H. Phan and J. Suzuki, "R2-IBEA: R2 indicator based evolutionary algorithm for multiobjective optimization," in *Evolutionary Computation (CEC), 2013 IEEE Congress on*. IEEE, 2013, pp. 1836–1845.

[17] R. H. Gómez and C. A. C. Coello, "MOMBI: A new metaheuristic for many-objective optimization based on the R2 indicator," in *Evolutionary Computation (CEC), 2013 IEEE Congress on*. IEEE, 2013, pp. 2488–2495.

[18] D. Brockhoff, T. Wagner, and H. Trautmann, "R2 indicator-based multiobjective search," *Evolutionary Computation*, vol. 23, no. 3, pp. 369–395, 2015.